

# Three-body interactions involving clusters and films

Silvina M. Gatica<sup>1</sup>, M. Mercedes Calbi<sup>1</sup>, Milton W. Cole<sup>1,3</sup>, and Darrell Velegol<sup>2</sup>

*Departments of Physics<sup>1</sup> and Chemical Engineering<sup>2</sup>, and Materials Research Institute<sup>3</sup>,  
Pennsylvania State University, University Park, PA 16802*

(Dated: June 19, 2018)

## Abstract

The three body (triple dipole) interaction of Axilrod, Teller and Muto (ATM) contributes 5 to 10 % of the total energy of condensed phases of inert elements. It is shown in this paper for clusters and films that a much larger or smaller ATM contribution can arise for other geometries or other atomic species. The ratio  $R$  of the three body interaction energy to the two body energy is evaluated for a wide variety of configurations. This ratio varies considerably with the geometry. For highly polarizable atoms in certain geometries, the magnitude of the three body energy is comparable to that of the two body energy and can be either attractive or repulsive. Systematic trends are established and explained.

## I. INTRODUCTION

The growing interest in problems involving interfaces has stimulated a large literature involving computations of the properties of such systems<sup>1,2</sup>. Most of these studies have assumed that the potential energy of the system is well approximated by a sum of two-body interactions between pairs of the constituent particles. In some of these instances, the pair potentials are not well known, so the implicit or explicit neglect of many-body interactions is appropriate, in view of the manifest quantitative limitations of these particular calculations. In some other cases, however, the pair potentials employed in the calculations have been constructed from empirical fits to properties of the relevant bulk systems; some authors have suggested that such potentials inherently include higher order, many-body contributions<sup>3,4</sup>. Implicit in the latter point of view is the assumption that the many-body interactions in the given problem are of a similar form and magnitude to those in the bulk system. That assumption is evidently worth assessing in those cases where it can be tested. In this paper, we explore the importance of three-body van der Waals (VDW) interactions between a single atom and clusters of varying sizes and shapes, from nearly spherical to flat. In all cases, the atoms in the cluster are located at sites of a lattice of lattice constant  $a$ , like that shown in Fig. 1. Our study leads us to conclude that one should *not* expect three-body interactions to be properly reckoned when an empirical pair potential is employed.

Our analysis of the three-body energy is based on the Axilrod-Teller-Muto (ATM) expression for that energy<sup>5,6</sup>. For specificity, we consider the case when all three atoms are identical; then the interaction may be written:

$$V_{ATM}(\mathbf{r}_1, \mathbf{r}_2, \mathbf{r}_3) = \frac{9}{16} \frac{E_a \alpha_0^3}{r_{12}^3 r_{23}^3 r_{13}^3} (1 + 3 \cos \theta_1 \cos \theta_2 \cos \theta_3) \quad (1)$$

In this expression, the three angles represent the inner angles of the triangle connecting the atoms (which has sides of length  $r_{12}$ ,  $r_{13}$  and  $r_{23}$ ), the quantity  $\alpha_0$  represents the static polarizability of the atom and  $E_a$  is an energy (of order the ionization energy) characterizing the assumed frequency dependence of the polarizability at imaginary frequency:

$$\alpha(i\omega) = \frac{\alpha_0}{1 + (\frac{\hbar\omega}{E_a})^2} \quad (2)$$

Representative values of these parameters for some atoms appear in Table I.

The preceding ATM expression is a dispersion interaction, derived from third-order perturbation theory, ignoring exchange and overlap of the three atoms' wave functions; thus, it

is known to be valid at large separation, where “large” means relative to the atom’s hard-core interaction diameter. Empirical studies have often employed the interaction at closer approach but there is some disagreement about the validity of such applications<sup>8,9,10,11</sup>; proposals have been presented that modify the behavior at small separation<sup>12</sup>. That important question is beyond the scope of the present work. The origin of the ATM interaction is not particularly intuitive. For that reason, among others, we discuss in Appendix A its origin in a particularly simple limit: the case when one atom (A) is far from the other two (B and C). In the limit when the characteristic frequency of A is much less than that of B and C, the three body (ATM) energy coincides with the mean electrostatic interaction between dipoles induced on B and C by the dipolar fluctuations of A.

The outline of this paper is the following. Section II presents a study of the VDW interactions between an atom and a monolayer film, from which we make a straightforward extension to include the case of an entire 3D crystal. Section III describes the three-body interactions between an atom and a cluster of atoms. It will be shown in both of these sections that the three-body energy  $V_3$ , relative to the two-body energy  $V_2$ , is proportional to the product  $n_s\alpha_0$  of the number density of the solid and the polarizability (Table 1). Because of this dependence, we focus our attention on a dimensionless ratio

$$R = \frac{V_3}{V_2} \frac{1}{n_s\alpha_0} \quad (3)$$

$R$  depends very much on the specific geometry and can be either positive or negative. In particular,  $R$  has a drastically different dependence on separation in the two problems investigated here. In the cluster case, the ratio decreases with distance (vanishing at large distance) while in the atom-solid case, the magnitude of  $R$  increases with distance, asymptoting to a constant value that may be derived from the continuum theory of VDW interactions. For reference, we state the corresponding result in the case of the cohesive energy of inert gas solids; the ratio of three-body to two-body energies then is typically less than 10 per cent<sup>10,11</sup>. This small value reflects in part a significant cancellation of ATM terms of opposite sign in a bulk material. The present study finds similar cancellation in some geometries, but not others. In the latter case, the three-body energy represents an important term that should be included in calculations of system properties. Section IV discusses the implications of this work.

## II. THREE-BODY ATOM-MONOLAYER AND ATOM-SOLID INTERACTIONS

It was shown by Dzyaloshinskii, Lifshitz and Pitaevski<sup>13</sup> that the long range interaction between a nonpolar atom<sup>14</sup> at position  $\mathbf{r}=(0,0,z)$  and a semi-infinite solid, that occupies the half-space  $z < 0$ , assumes the form

$$V(\mathbf{r}) \sim -\frac{C_3}{z^3} \quad (4)$$

$$C_3 = \frac{\hbar}{4\pi} \int d\omega G(\omega) \alpha(i\omega) \quad (5)$$

Here  $G(\omega)$ , the surface-response function at imaginary frequency, is determined from the dielectric function  $\varepsilon(i\omega)$

$$G(\omega) = \frac{\varepsilon(i\omega) - 1}{\varepsilon(i\omega) + 1} \quad (6)$$

Among the questions addressed in this section is the relative importance of contributions to  $C_3$  from pair interactions and three-body interactions; we call these contributions  $C_3^{(2)}$  and  $C_3^{(3)}$ , respectively. We first consider the problem of an atom situated at position  $\mathbf{r}=(0,0,z)$  interacting with a square lattice ( $s \times s$ ) of atoms that comprise a monolayer film, in the  $z = 0$  plane; its crystalline lattice directions are oriented along the  $x$  and  $y$  axes. In this case, the two-body van der Waals interaction may be written:

$$V_2 = -\sum_i \frac{C_6}{r_i^6} \quad (7)$$

Here, the sum is over all atoms ( $i$ ) of the film, each at distance  $r_i$  from the external atom, and the coefficient of the asymptotic VDW pair interaction is

$$C_6 = \frac{3}{4} E_a \alpha_0^2 \quad (8)$$

This expression (first obtained by London<sup>15</sup>) is derived from the frequency-dependent polarizability, Eq. (2). For  $s = 60$ , Fig. 2 presents the dimensionless two-body potential

$$U_2 = \frac{V_2}{\epsilon_2} \quad ; \quad \epsilon_2 = E_a (\alpha_0 n_s)^2 \quad (9)$$

Similarly, we define

$$U_3 = \frac{V_3}{\epsilon_3} \quad ; \quad \epsilon_3 = \epsilon_2 \alpha_0 n_s \quad (10)$$

Values of  $\epsilon_2$  and  $\epsilon_3$  are presented in Table I. One observes a significant dependence of the energy on lateral position only at small  $z/a$ , since at  $z > a$  the film looks continuous. At large distance, one finds for  $V_2$  a result that can be derived from an integration over the monolayer, which has a two-dimensional (2D) density  $1/a^2$ :

$$V_2(\mathbf{r}) \sim -\frac{C_{mono}^{(2)}}{z^4} \quad ; \quad C_{mono}^{(2)} = \frac{\pi}{2} \frac{C_6}{a^2} \quad (11)$$

The superscript (2) in the coefficient indicates that this energy originates from the pair interactions, i.e. Eq. (7). Also shown in Fig. 2 is the total three-body energy, obtained by summing ATM interactions between all pairs of atoms in the monolayer and the external atom (at  $\mathbf{r}$ ):

$$V_3(\mathbf{r}) = \sum_{i < j} V_{ATM}(\mathbf{r}_i, \mathbf{r}_j, \mathbf{r}) \quad (12)$$

This energy is positive because the contribution of the repulsive terms in the sum exceed those of attractive terms. In Fig. 3 we show the ratio  $R$  (Eq. (3)) for this case. One observes in the inset of this figure that at a distance  $z$  much larger than the lattice constant  $a$  (but smaller than the monolayer's lateral extent) the ratio of these interactions is  $R_{monolayer} \approx -1.6$ . We will derive this result below. For distances larger than the size of the monolayer (equal to  $60a$  in the case of the Fig. 3), the value of  $(V_3/V_2)$  approaches a finite value that depends on the size of the monolayer. This value is discussed in the next section.

Now, let us address the problem of the three-body interaction in the case of an atom above a half-space solid, consisting of layers located at  $z = -na$ , where  $n = 0, 1, 2, \dots$ . First, we evaluate the two-body contribution by summing the monolayer energy over all layers. We note, from the Euler-Maclaurin theorem and Eq. (11), that the asymptotic dependence is

$$V_2(\mathbf{r}) \sim -C_{mono}^{(2)} \sum_n \frac{1}{(z + na)^4} \sim -\frac{\pi}{6} n_s \frac{C_6}{(z - \frac{a}{2})^3} \quad (13)$$

This leads to the result that the two-body contribution to the asymptotic potential of Eq. (4) involves a coefficient

$$C_3^{(2)} = \frac{\pi}{6} n_s C_6 \quad (14)$$

We now evaluate the analogous three-body asymptotic coefficient,  $C_3^{(3)}$ . The expression is obtained from Eq. (12), with the sum of the ATM interactions taken over pairs of atoms throughout the half-space  $z \leq 0$ . To determine this quantity requires consideration of two-kinds of terms in the sum, leading to:

$$V_3 = V_3^{inter} + V_3^{intra} \quad (15)$$

The interlayer term  $V_3^{inter}$  represents the three-body contribution arising from pairs of solid atoms coming from different planes, while the intralayer term  $V_3^{intra}$  involves pairs of atoms from the same plane. Fig. 4 shows the resulting  $R^{inter}$  and  $R^{intra}$  terms.

In Appendix B, we prove that the first term in Eq. (15) is identically zero at large separation, leaving just the second term. We note that the ratio of this surviving intralayer term to the analogous pair interaction term was calculated above for a single layer, as shown in Fig. 3; the ratio asymptotes to a constant value mentioned above. This means that, in the semi-infinite solid case, the same ratio applies to contributions from all planes, leading to exactly the same asymptotic ratio for the solid and the monolayer. Thus, asymptotically,

$$\left(\frac{V_3}{V_2}\right)_{solid} \sim \frac{C_3^{(3)}}{C_3^{(2)}} \sim -1.6 n_s \alpha_0 \quad (16)$$

We now explain why this numerical result arises (and could have been anticipated without any numerical calculations). To do so, we employ the Clausius-Mossotti relation:

$$\frac{\varepsilon(i\omega) - 1}{\varepsilon(i\omega) + 2} = \frac{4\pi}{3} n_s \alpha(i\omega) \equiv \xi(i\omega) \quad (17)$$

Assuming that the quantity  $\xi$  is small (the case of small  $V_3/V_2$ ), we may expand the relation for the asymptotic VDW coefficient, Eq. (5):

$$C_3 = \frac{\hbar}{4\pi} \int d\omega \alpha(i\omega) \left[ \frac{3}{2} \xi(i\omega) \left( 1 - \frac{\xi(i\omega)}{2} \dots \right) \right] \quad (18)$$

$$C_3 = C_3^{(2)} + C_3^{(3)} \dots \quad (19)$$

The identification of successive terms with increasing number of interacting particles is physically plausible and is demonstrated here for the first two terms. If one inserts into these equations the Drude expression for the polarizability, Eq. (2), assuming the same species for external atom and solid atoms, one obtains

$$C_3^{(2)} = \frac{\hbar}{2} n_s \alpha_0^2 \int d\omega \frac{1}{\left[1 + \left(\frac{\hbar\omega}{E_a}\right)^2\right]^2} \quad (20)$$

$$C_3^{(3)} = -\frac{\hbar\pi}{3} n_s^2 \alpha_0^3 \int d\omega \frac{1}{\left[1 + \left(\frac{\hbar\omega}{E_a}\right)^2\right]^3} \quad (21)$$

The integrals may be evaluated, leading to values of the two relevant contributions to the dispersion coefficient:

$$C_3^{(2)} = \frac{\pi}{8} n_s \alpha_0^2 E_a = \frac{\pi}{6} n_s C_6 \quad (22)$$

$$C_3^{(3)} = -\frac{\pi^2}{16} n_s^2 \alpha_0^3 E_a \quad (23)$$

The ratio of coefficients results:

$$\frac{C_3^{(3)}}{C_3^{(2)}} = -\frac{\pi}{2} n_s \alpha_0 \quad (24)$$

This result is fully consistent with the behavior found numerically, with coefficient  $R = -\pi/2 \approx -1.6$ , Eq. (16). This confirms our attribution of the physical origin of the first two terms in the expansion of  $C_3$ .

We also explore the dependence of  $V_3$  on the orientation of the monolayer. This is shown in Fig. 5. The result is that  $V_3$  depends very strongly on the orientation, becoming attractive when the single atom and the monolayer are coplanar. The origin of this behavior will be explained in the next section.

### III. THREE-BODY INTERACTION BETWEEN A SINGLE ATOM AND A CLUSTER

Now, we address the problem of a single atom at a distance  $z$  from a quasi-spherical cluster. By ‘‘quasi-spherical’’ we mean a cluster of  $N$  atoms constructed from the closest

$N$  points to the center of a simple cubic lattice of sites. The resulting ratio  $R$  in this configuration is shown in Fig. 6 for different sizes and orientations of the cluster. There are at least three particularly interesting dependences seen in this figure. The first is that  $R$  goes asymptotically to zero, in contrast to the nonzero constant value in the case of a monolayer at large distance. The second is the presence of a maximum in the magnitude of  $R$ . A third is that  $R$  depends strongly on the orientation of the cluster. For example, in the case of the clusters with 7 and 33 atoms, the three-body interaction is attractive for  $\theta = 0$  but repulsive for large values of  $\theta$ . In the other two cases shown in this figure (clusters with 19 and 93 atoms), the trend is reversed.

We now explain why  $R$  vanishes at large  $z$  for quasi-spherical clusters. The ATM expression Eq. (1) at large  $z$  is simplified because two of the three interatomic distances are essentially equal to  $z$  and two of the interior angles of the three-atom triangle sum to  $\pi$ , while the third angle nearly vanishes. Then, the energy may be written

$$V_{ATM}(z) = \frac{C}{z^6} \sum_{i < j} \frac{(1 - 3 \cos^2 \phi_{ij})}{r_{ij}^3} \quad ; \quad C = \frac{9}{16} E_a \alpha_0^3 \quad (25)$$

Here, the sum is over pairs of atoms in the cluster, separated by distance  $r_{ij}$  and  $\phi_{ij}$  is the angle between their separation vector  $\mathbf{r}_{ij}$  and the vector connecting the atoms to the external atom. Since the term in parentheses can vary between (-2) and 1, the sign of the resultant sum is not obvious. However, in a case where the separation vectors are randomly oriented, the average value of  $\cos^2 \phi$  is 1/3. Similarly, for an *infinite* simple cubic lattice, the average is 1/3, as may easily be established (for any crystalline orientation). In either of these cases, therefore, the sum in Eq. (25) vanishes identically. In the case of a finite quasi-spherical cluster, the ATM sum is nonzero, due to residual surface contributions, but it is small compared to the two-body energy, which is proportional to the number of atoms in this large separation limit. Thus, it is expected that  $R$  should be very small for symmetric clusters at large distances.

To understand the intriguing angular dependence in Fig. 6, we undertake additional calculations, as follows. We consider the long range interaction for two geometries shown in Fig. 7. In Fig. 7(a) appears the interaction for anisotropic clusters consisting of ( $s=1,2$  or 3) rows of atoms, with  $N$  atoms per row, oriented parallel to the  $z$  axis, on which the atom is located. One observes for  $s = 1$  row that  $R$  is positive ( $V_3 < 0$ ) for all values of  $N$ . This

behavior can be understood readily from Eq. (25) because  $\phi_{ij} = 0$  for all pairs within the cluster. Hence, every term is negative and the sum increases essentially linearly with the number of nearest neighbor pairs (and hence  $N$ ) for  $z/a \gg N$ . Cases involving  $s > 1$  yield somewhat less attractive ATM sums, relative to two-body sums, as indicated in the  $s = 2$  and 3 curves in Fig. 7(a). To summarize, needle-like clusters, pointed toward the external atom, have negative ATM interactions, enhancing the two-body attraction.

What about more symmetric structures? In Fig. 7(b), we show results for systems consisting of atoms located at the sites of  $N$  parallel squares of size  $s$ . The distance from the external atom to the first square is  $z = 10s$ , and  $R$  is plotted as a function of  $N/s$ . We see that for  $N/s < 1$  the 3-body contribution is repulsive, while for  $N/s > 1$  it is attractive. In the case  $N/s = 1$ , that corresponds to a cubic configuration, the ratio  $R$  is almost zero at this distance. Thus, the asymptotic behavior of the cube is analogous to that of the small clusters. We note from Fig. 7 that this vanishing is an “accident”, in that nonzero values of opposite signs occur for  $N > s$  or  $N < s$ .

Now suppose, instead, that our system consists of atoms on sites of three parallel squares, as in Fig. 8. As expected, if the side of the squares is exactly 3,  $R$  goes to zero, while the asymptotic value of  $R$  becomes finite (and negative) for  $s > 3$ . Note that this trend is consistent with the asymptotic value  $R \approx -3.1$  for one layer, with  $s = 60$ , shown in Fig. 3, and can be understood by the following argument. At large  $z$  ( $\gg sa$ ), the film atoms are essentially equidistant from the external atom. Hence, the two-body energy is  $V_2 = -NC_6/z^6$ . As for the ATM energy, in the case of normal incidence at large  $z$ , the term involving 3 cosines in Eq. (1) vanishes, leaving:

$$V_{ATM} = \frac{9}{16} E_a \alpha_0^3 \Sigma \quad (26)$$

The sum  $\Sigma$  is over all pairs of atoms; for a film of very large extent, this may be written

$$\Sigma = \sum_{i < j} \frac{1}{r_{ij}^3} \equiv N_a \frac{k}{a^3} \quad ; \quad (N_a \gg 1) \quad (27)$$

Here,  $N_a$  is the total number of atoms and  $k = 4.7$  is a numerical factor evaluated from the sum. Since  $C_6 = (3/4)E_a\alpha_0^2$ , the ratio  $R$  becomes

$$R = -\frac{3}{4}k \approx -3.5 \quad (28)$$

The large  $z$ , large  $s$ , limit of Fig. 3 approaches this value. For large  $z$ , but  $s$  not very large compared to 1, the contribution of sites on the boundary of the film causes  $\Sigma$  to be less than  $Nk/a^3$ , so the ratio  $R > -3.5$  (as seen in Fig. 8). This is a significant reduction in magnitude for finite  $s$  because the fraction of sites on the border of an  $s \times s$  square is  $4(s - 1)/s^2$ .

These results lead to a relatively simple and comprehensive picture of the role of three-body interactions. Lines of atoms pointing toward the external atom lead to attraction, while planes of atoms perpendicular to the cluster-atom separation vector lead to repulsive interactions overall (see Appendix A). Note, in particular, that the explanation clarifies the peculiar angle-dependence in Fig. 6. In the process of making the clusters nearly spherical, those with  $N = 7$  and 33 end up with single atom prominences on their external "faces". The  $N = 7$  cluster consists of an atom at the origin and one along each of the  $+/-$  axes. The  $N = 33$  cluster is composed by a cube of side 3 plus an additional atom at the center of each face. In particular, when  $\theta = 0$  these configurations mimic the effect of a line of atoms pointing toward the external atom originating an attractive interaction as indicated by the dashed lines in the left panels of Fig. 6. Instead, the other two clusters with  $N = 19$  or 93 face the external atom with an almost complete plane of atoms perpendicular to the cluster-atom separation vector, leading to repulsive interactions at small angle  $\theta$  (dashed lines in right panels of Fig. 6).

#### IV. DISCUSSION AND FINAL REMARKS

The calculations in this paper use the Axilrod-Teller-Muto three-body interaction to supplement the contribution from two-body calculations of van der Waals dispersion forces. Specific calculations reveal that material geometry - both the morphology and orientation of clusters - is important, and that changing the orientation of a cluster can cause the overall VDW potential to change from attractive to repulsive. This is especially true for clusters with high polarizability.

Our calculations suggest three heuristics for predicting van der Waals dispersion interactions between an atom A and a material B (e.g., surfaces, clusters, or atoms) interacting by a force along a unit vector  $\hat{e}$ : 1) If B has a large dimension perpendicular to  $\hat{e}$ , this tends to produce a repulsive 3-body force with A, thus reducing the total dispersion attractions; 2)

if B has a large dimension parallel to  $\hat{e}$  (i.e., depth), this tends to produce attractive 3-body forces with A, thus increasing the total dispersion attractions; 3) if B is quasi-spherical, this tends to decrease the magnitude of 3-body forces with A, meaning that the pairwise interaction sum gives a good approximation to the total interaction.

This work has produced other important conclusions as well. For example, in assessing 3-body interactions between an atom and a semi-infinite solid, only the intra-plane contributions to the 3-body effect are important; that is, distinct layers of the solid do not interact significantly with the external atom to produce 3-body ATM effects. In addition, analytical calculations show that the 3-body effect asymptotes to zero for quasi spherical clusters, as opposed to semi-infinite materials.

At least two interesting questions arise from this work. First, since we did not assess 4-body interactions, it remains to be seen whether 4-body interactions are of the same order of magnitude as 3-body interactions. Presumably such interactions scale as one higher power of the expansion parameter  $n_s\alpha_0$ . Second, the effect of coating layers on particles can be examined by a similar methodology. In 2-body effects only, the coating layer might not alter the VDW forces significantly; however, based on the present work, the 3-body forces could produce even repulsive net interactions.

### **Acknowledgments**

We are grateful to L.W. Bruch for stimulating and helpful discussions. This research has been supported by the National Science Foundation, the Ben Franklin Technology Center and the Environmental Protection Agency.

### **APPENDIX A: NATURE OF THE ATM INTERACTION AT LARGE DISTANCE**

In this section we explore the microscopic nature of the ATM interaction by deriving its form (in a particular case) using a distinct *alternative* to the conventional approach to deriving the three-body interaction. The method described here provides a simple interpretation to this energy that is consistent with the general notion that such dispersion interactions arise from interactions between fluctuating dipole moments.

To be specific, we consider the situation when two atoms (B and C) are close together while the third atom (A) is located at large distance from the pair. Furthermore, for convenience, we make a specific assumption about the values of their characteristic energies that is different from that used to derive Eq. (1). The latter assumes that all three energies are the same; here, instead, we assume that  $E_A$ , the characteristic energy of atom A, is small compared to the energies (both  $E'$ ) of B and C, meaning that A has a slowly fluctuating dipole moment. In this limit, we evaluate the triple dipole interaction by setting it equal to the electrostatic interaction between the two instantaneous dipoles (on B and C) that are induced by dipolar fluctuations of the third atom, A.

Assume that the external atom (A) is located at the origin and the B, C pair of atoms is located at distance  $z$  on the  $z$  axis. A dipole moment fluctuation  $\mathbf{p}$  on A will produce an electric field  $\mathbf{E} = [-\mathbf{p} + 3p_z\hat{\mathbf{z}}]/z^3$  at the neighboring positions of the B, C pair, where  $\hat{\mathbf{z}}$  is the unit vector in the  $z$  direction. Atoms B and C polarize instantaneously (in comparison with A), so that they develop an identical induced dipole moment  $\mathbf{p}_{induced} = \alpha_0\mathbf{E}$ . The electrostatic interaction energy between two such dipoles is then obtained in the usual way, resulting in:

$$\langle E_{BC} \rangle = \frac{\alpha_0^2}{z^6} \langle \mathbf{p}^2 \rangle_A \frac{(1 - 3 \cos^2 \phi_{BC})}{r_{BC}^3} \quad (\text{A1})$$

Here, we have averaged over the time-dependent fluctuations of  $\mathbf{p}$  on atom A, with the average denoted by brackets. The angle  $\phi_{BC}$  is that between the BC separation vector and the AB separation vector. Note that this energy is usually nonzero, varies as the inverse cube of the B-C separation and the inverse sixth power of the distance to A and has an interesting angle dependence. To explore the comparison with Eq. (1), we evaluate  $\langle \mathbf{p}^2 \rangle_A$  within the Drude approximation<sup>16</sup>, Eq. (2). The result is  $\langle \mathbf{p}^2 \rangle_A = (3/2)E_A\alpha_0$ . Hence, we arrive at the expression for the three-body interaction in this approximation:

$$V(z) = \frac{3}{2} E_A \frac{\alpha_0^3}{z^6} \frac{(1 - 3 \cos^2 \phi_{BC})}{r_{BC}^3} \quad (\text{A2})$$

With one exception, this equation coincides with the result obtained from Eq. (1) in the present geometry (two angles summing to  $\pi$  and the third vanishing). The exception is the value of the numerical coefficient, which is here  $(3/2)$  instead of  $(9/16)$  in Eq. (1). This difference arises because Eq. (1) is obtained from the ATM model for a case when the

characteristic energies coincide, while Eq. (A1) assumes that the energies are very different,  $E_A \ll E'$ . If this latter set of energies were inserted in the *general* ATM expression, it would yield the same (3/2) coefficient found here. Thus, we have identified a plausible and intuitive explanation (induced dipole interactions) of the origin of this ATM interaction and shown that the energy computed in the present limit agrees with ATM formula in the case of the same interacting atoms.

## APPENDIX B: INTERLAYER THREE-BODY INTERACTION

The total interlayer ATM interaction for an atom above a half-space crystal may be written as a sum of terms in which the external atom (0) is fixed in position and one sums over all pairs of internal atoms. We evaluate the sum by considering a particular individual atom ( $i$ ) within the solid and summing over atoms in all layers below it, which we represent as a continuum. McLachlan evaluated the many-body interaction for precisely this geometry<sup>17,18</sup>, depicted in Fig. 9. Atom  $i$  lies at distance  $b$  (of order a lattice constant) above the continuum while the external atom lies at distance  $h = z + na + b$  above this continuum; here  $n$  is the layer number for atom  $i$ . The atoms labelled 0 and  $i$  are separated laterally by a distance  $R$ . McLachlan's resulting expression for this many-body interaction energy involves two coefficients:

$$C_{s1} = \frac{3\hbar}{\pi} \int \xi(i\omega) \alpha^2(i\omega) d\omega \quad (\text{B1})$$

$$C_{s2} = \frac{3\hbar}{\pi} \int \xi^2(i\omega) \alpha^2(i\omega) d\omega \quad (\text{B2})$$

Since the first of these coefficients is proportional to the third power of the polarizability, it represents a contribution to the three-body energy explored in this paper. The  $C_{s2}$  coefficient is of fourth order in the polarizability, as discussed explicitly below. Corresponding to these coefficients, the expression of McLachlan yields a limiting behavior, for  $h \gg b$ , as follows:

$$V_M = C_{s1}U_1(R, z) + C_{s2} \frac{1}{(R^2 + h^2)^3} \quad (\text{B3})$$

$$U_1(R, z) = \frac{1}{(R^2 + h^2)^3} \left[ \frac{4}{3} - \frac{2h^2}{R^2 + h^2} \right] \quad (\text{B4})$$

Note that the  $U_1$  term is negative for  $R/h < 2^{-1/2}$  and positive for larger  $R/h$ , with a maximum at  $R = h$ . Hence, there tends to be cancellation between these regimes of distance.

To determine the total contribution from all of the atoms in layer  $n$ , we need to sum this expression for  $V_M$  over a monolayer of atoms; for  $h \gg b$ , we can achieve this by integrating this term over all positions  $\vec{R}$  in the plane of atom  $i$ . Note that

$$\int U_1(R, z) d^2 \vec{R} = 0 \quad (\text{B5})$$

We conclude that the three-body contribution from interlayer interactions vanishes at large distance. The remaining interlayer contribution is fourth order, which is not considered in this paper. For completeness, however, we evaluate this contribution from layer  $n$ , of two-dimensional density  $1/a^2$ :

$$V_{4n} = \frac{1}{a^2} \int \frac{C_{s2}}{(R^2 + h^2)^3} d^2 \vec{R} = -\frac{\pi C_{s2}}{2} \frac{1}{a^3 h^4} \quad (\text{B6})$$

We may then integrate this contribution over all of the layers ( $n$ ), yielding

$$V_{4inter} = -\frac{\pi C_{s2}}{6} \frac{1}{a^2 z^3} \quad (\text{B7})$$

The ratio of this term to the two-body term is found to be

$$\frac{V_{4inter}}{V_2} = \frac{C_{s2}}{C_6} = \frac{5}{8} \left( \frac{2\pi\alpha_0}{a^3} \right)^2 \quad (\text{B8})$$

This is smaller by a factor  $\sim \alpha_0/a^3$  than the corresponding ratio in Eq. (14), for the three-body intralayer term. We note, however, that we have not considered fourth order intralayer terms, which might be larger and/or of opposite sign.

---

<sup>1</sup> L.W. Bruch, M.W. Cole and E. Zaremba, *Physical Adsorption: Forces and Phenomena*, Oxford U.P. (1997).

<sup>2</sup> H.T.Davis, *Statistical mechanics of phases, interfaces and thin films* (VCH, New York, 1996).

<sup>3</sup> M. K. Kostov, M. W. Cole, J. C. Lewis, P. Diep and J. K. Johnson, Chem. Phys. Lett. 332, 26-34 (2000).

<sup>4</sup> J.A. Barker, Phys. Rev. Lett. **57**, 230; see also section 5.3 of Ref. 2.

<sup>5</sup> B.M. Axilrod and E. Teller, J. Chem. Phys., **11**, 299 (1943).

<sup>6</sup> Y. Muto, Journal of the Physico-Mathematical Society of Japan **17**, 629 (1943).

<sup>7</sup> CRC Handbook of Chemistry and Physics, 67th. ed. (1986).

Atom	$\alpha_0$ ( $\text{\AA}^3$ )	$\alpha_0 n_s$	$E_a$ (eV)	$\epsilon_2$ (eV)	$\epsilon_3$ (eV)
$^4\text{He}$	0.205	0.0045	24.59	$5 \times 10^{-4}$	$2 \times 10^{-6}$
Ar	1.64	0.041	15.76	0.026	0.001
C	1.76	0.176	11.26	0.35	0.06
Xe	4.04	0.067	12.13	0.05	0.004
Si	5.38	0.269	8.15	0.59	0.16
Au	5.8	0.342	9.23	1.1	0.37
Pt	6.5	0.179	8.96	0.29	0.05
Pb	6.8	0.225	7.42	0.38	0.08
Ag	7.2	0.422	7.58	1.4	0.57
Cu	7.31	0.617	7.73	2.9	1.8
Al	8.34	0.502	5.99	1.5	0.76
Fe	8.4	0.706	7.87	3.9	2.8
Mg	10.6	0.457	7.65	1.6	0.73
Na	23.6	0.600	5.14	1.9	1.1
Ca	25	0.582	6.11	2.1	1.2
K	43.4	0.576	4.34	1.4	0.83

TABLE I: Static polarizability ( $\alpha_0$ ), polarizability times number density ( $\alpha_0 n_s$ ) and ionization potential ( $E_a$ ) of various atoms and corresponding solids (values taken from Ref. 7). The energies  $\epsilon_2 = E_a(\alpha_0 n_s)^2$  and  $\epsilon_3 = \epsilon_2(\alpha_0 n_s)$  are the scale units for  $V_2$  and  $V_3$  used in Fig. 2.

<sup>8</sup> M.J. Elrud and R.J. Saykally, Chemical Reviews **94**, 1975 (1994).

<sup>9</sup> M. Schmeits and A.A. Lucas, Progress in Surface Science **14**, 1 (1983).

<sup>10</sup> J.A. Barker, in *Simple molecular systems at very high density*, (ed. A. Polian, P. Loubeyre, and N. Boccara), pp. 331, Plenum, New York (1989).

<sup>11</sup> J.A. Barker, R.O. Watts, J.K. Lee, T.P. Schaefer and Y.T.Lee, Mol. Phys. **21**, 657 (1974).

<sup>12</sup> T.I. Sachse, K.T. Tang, and J.P. Toennies, Chem. Phys. Lett. **317**, 346 (2000).

<sup>13</sup> I.E. Dzyaloshinskii, E.M. Lifshitz, and L.P. Pitaevskii, Advances in Physics **10**, 165 (1961).

<sup>14</sup> If a molecule has a nonzero dipole moment  $\mathbf{p}$ , its interaction with a perfectly conducting surface assumes the form  $V_{perm} = -p^2(1 + \cos^2 \theta)/(16z^3)$ , where  $\theta$  is  $\cos^{-1}(\mathbf{p} \cdot \hat{z}/|\mathbf{p}|)$ . This can be

interpreted in terms of an effective  $C_3(\theta)$  which yields, after orientational averaging over  $\theta$ ,  $C_3^{perm} = p^2/12$ . If  $p = 9(12)$  Debye, for example,  $C_3^{perm}$  agrees with the dispersion value  $C_3$  of Ar (Xe) on this surface.

<sup>15</sup> F. London, *Zeitschrift für Physik* **63**, 245 (1930).

<sup>16</sup> U. Fano and J.W. Cooper, *Rev. Mod. Phys.* **40**, 441 (1968).

<sup>17</sup> A.D. McLachlan, *Proceedings of the Royal Society (London) A* **271**, 387 (1963).

<sup>18</sup> A.D. McLachlan, *Molecular Physics* **7**, 381 (1964).

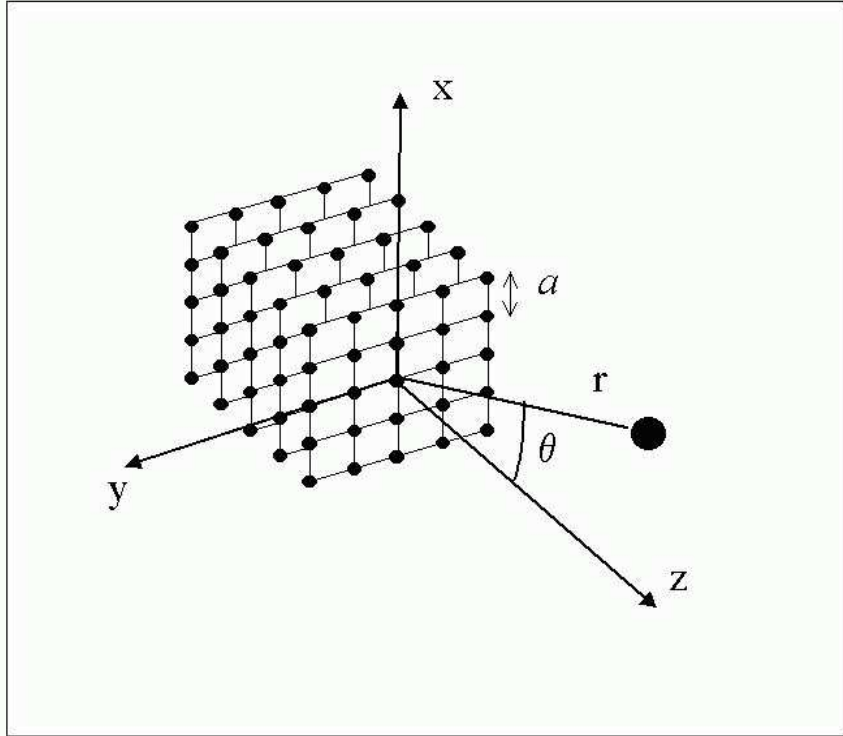


FIG. 1: Schematic picture of a cluster configuration of a five layer  $s \times s$  square array, with  $s = 5$  shown. The  $z$  axis is perpendicular to the layers that interact with the external atom at  $\mathbf{r}$ .

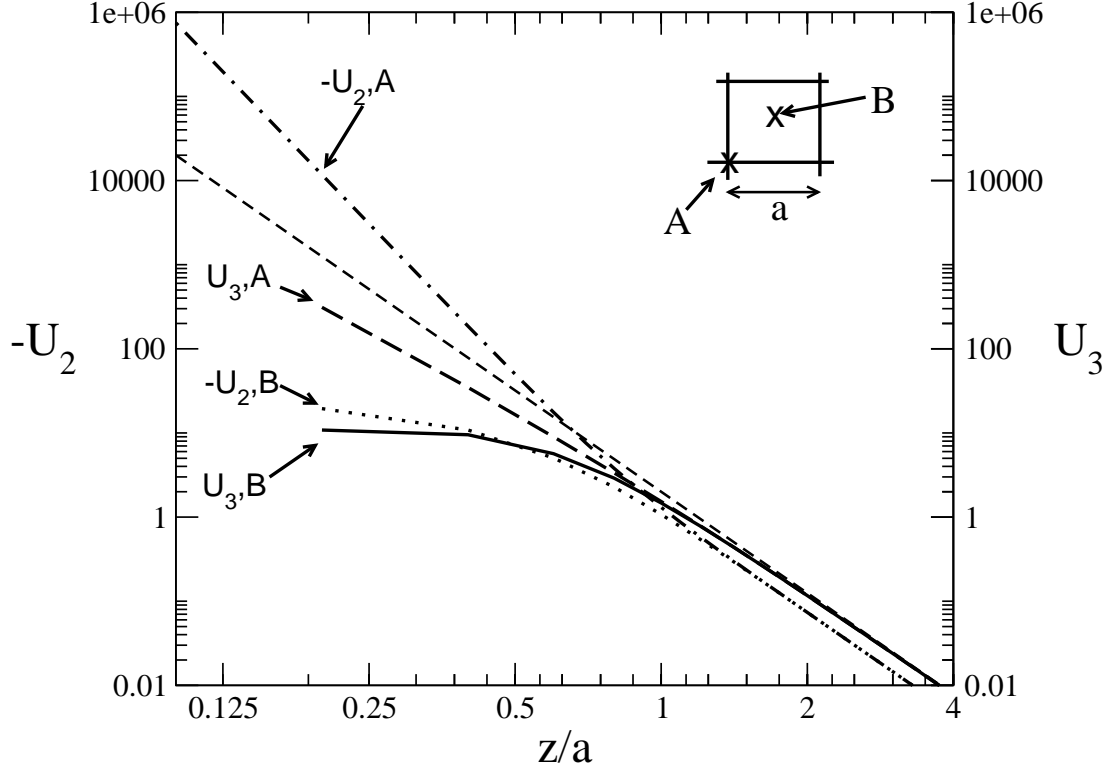


FIG. 2: Dimensionless two-body and three-body interactions  $U_2$  and  $U_3$  (defined in Eqs. (9) and (10)) for the case of an atom above a  $60 \times 60$  monolayer film as a function of perpendicular distance  $z/a$ , for two indicated values of the lateral position of the atom: above an atom of the film, A-top and above a midpoint of the square lattice of the film, B. The short-dashed line corresponds to the asymptotic  $z^{-4}$  prediction of Eq. (11).

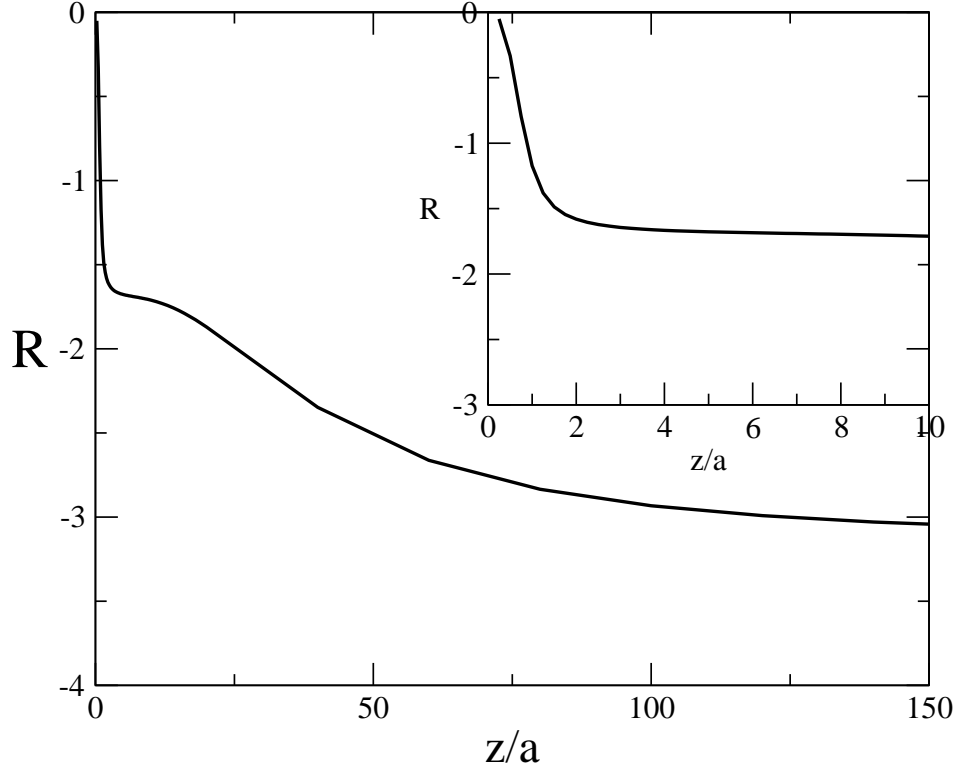


FIG. 3: Ratio  $R$ , defined in Eq. (3), of the three-body and two-body interaction between an atom at position  $(0,0,z)$  and a  $60 \times 60$  monolayer film, as a function of the perpendicular distance  $z$ . In the inset is shown an enlargement of the region of small  $z < 10a$ .

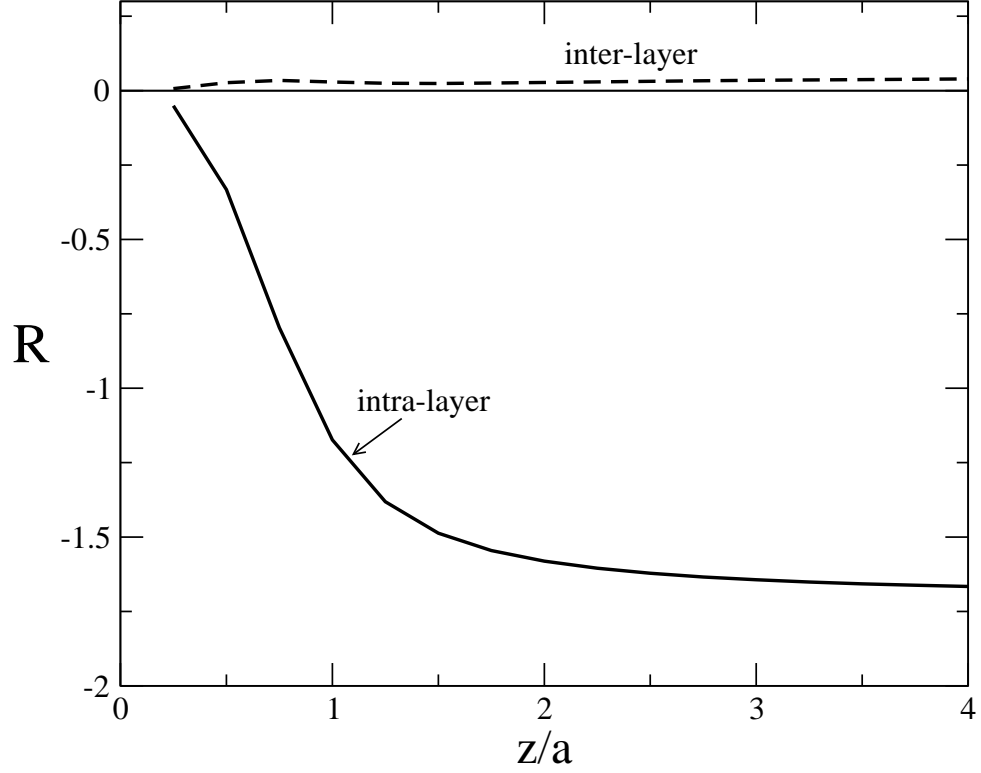


FIG. 4: Inter-layer and intra-layer contributions to the ratio  $R$  for an atom above a bilayer film.

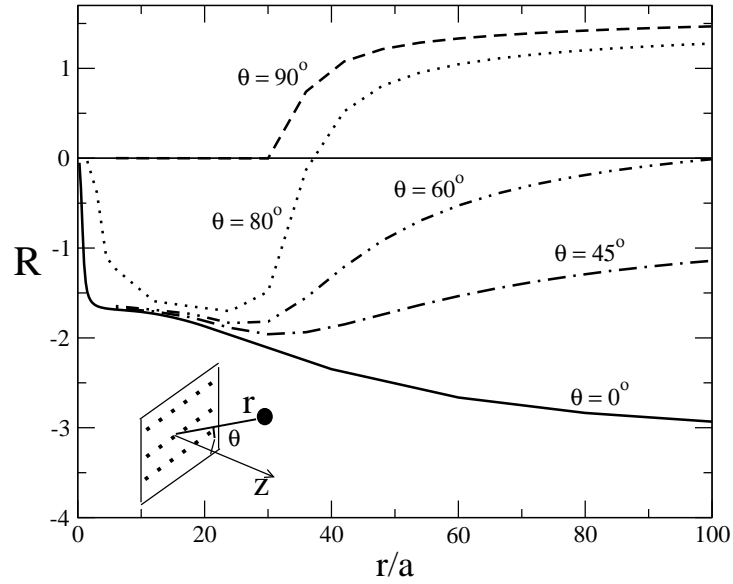


FIG. 5: Ratio  $R$  as a function of the distance  $r$  to the center of the  $60 \times 60$  monolayer for different orientations  $\theta$ .

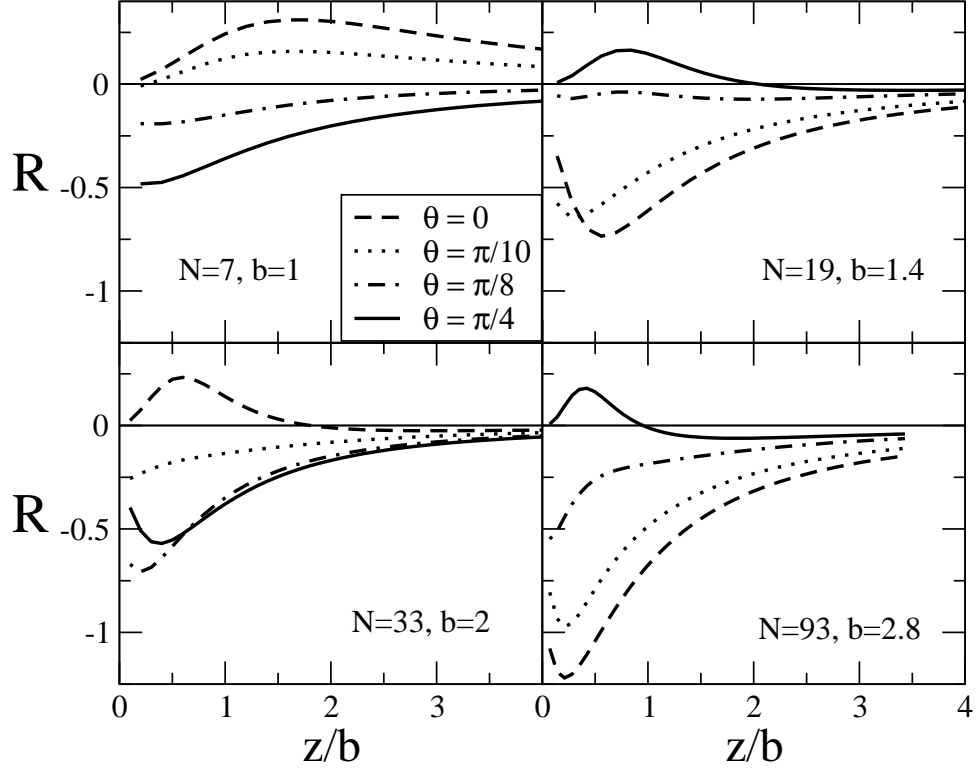


FIG. 6: Ratio  $R$  of the three-body to two-body interactions between an atom and a quasi-spherical cluster of radius  $ba$  as a function of the distance to the surface of the cluster, for different orientations  $\theta$ .  $N$  is the number of atoms in the cluster.

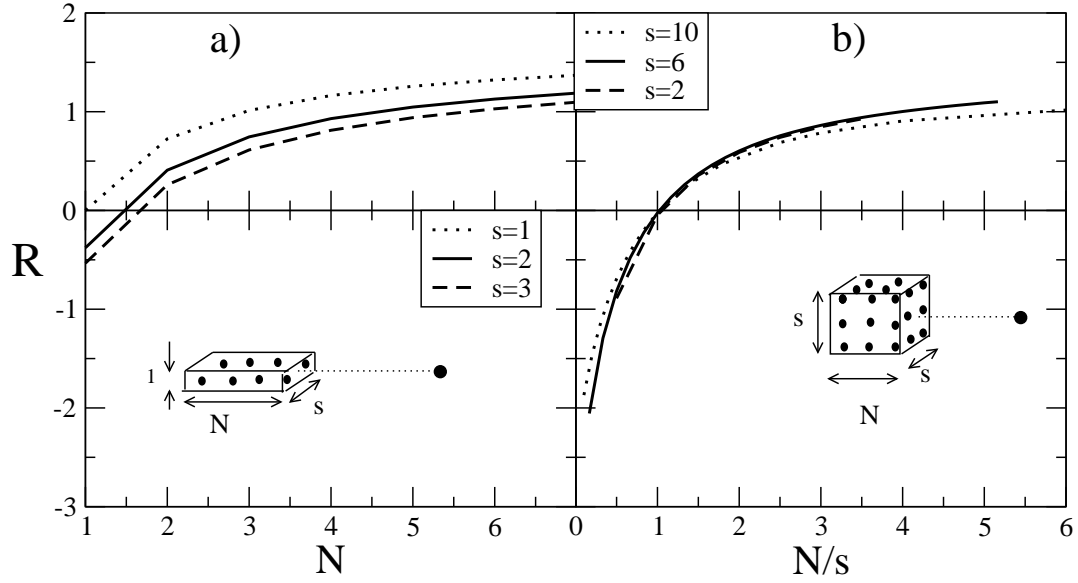


FIG. 7: (a) Ratio  $R$  evaluated at a distance  $z = 10a$ , for the case of an atom and a cluster of atoms in one line, two lines and three lines, as a function of the number of atoms in the line,  $N$ . (b) Ratio  $R$ , evaluated at a distance  $z = 10s$ , for the case of an atom and a cluster of atoms of dimension  $s \times s \times N$ .

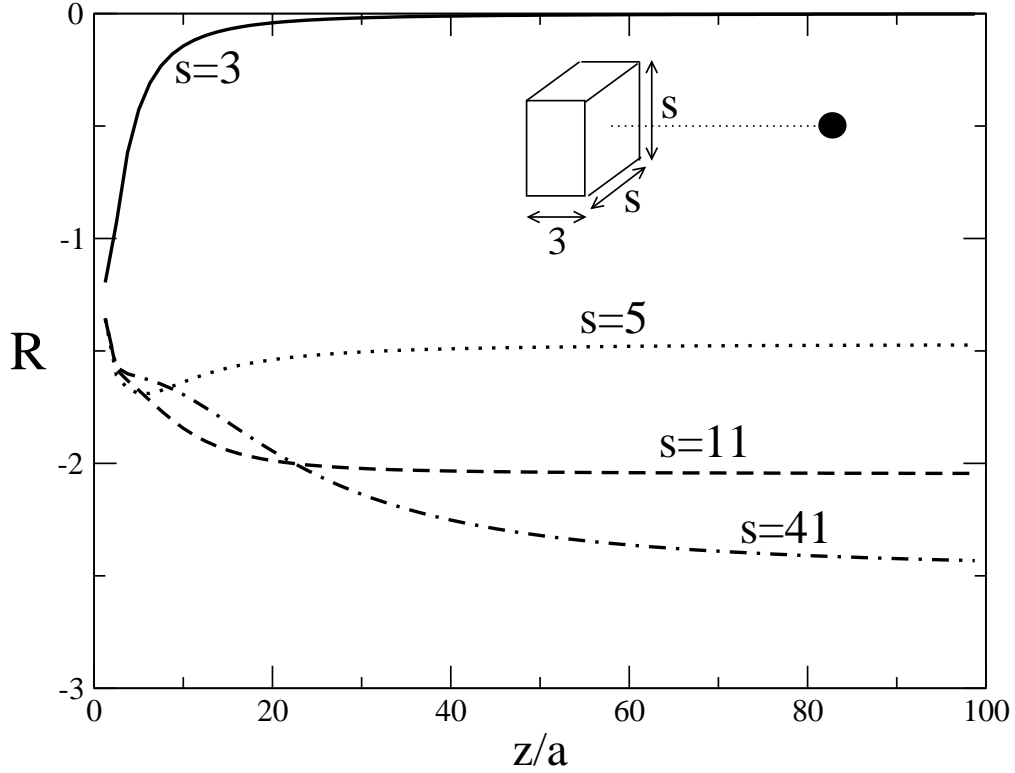


FIG. 8: Ratio  $R$  for the case of an atom and an  $s \times s \times 3$  cluster of atoms, as a function of the perpendicular distance  $z/a$ .

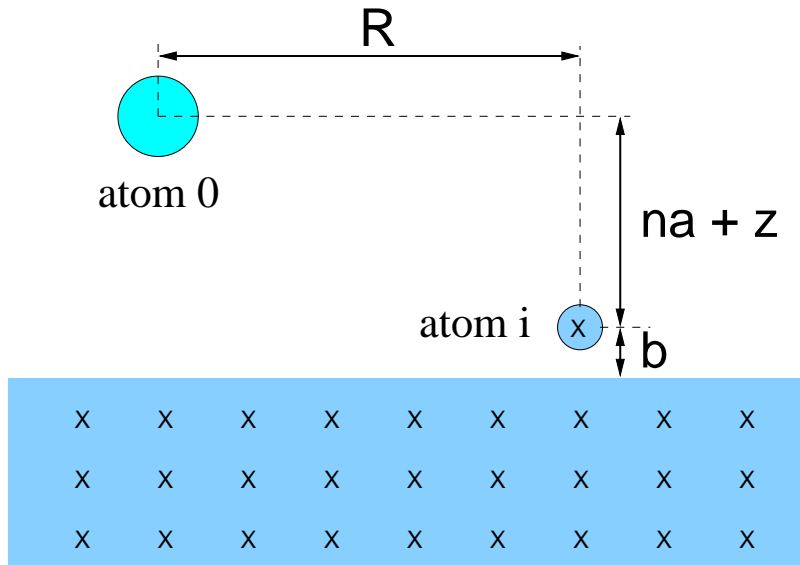


FIG. 9: The geometry corresponding to atoms 0 and i above a half-space, whose interaction is mediated by the solid below. The crosses represent the lattice structure of the solid.